J Ind Microbiol Biotechnol (2013) 40:735–747
DOI 10.1007/s10295-013-1269-3

METABOLIC ENGINEERING AND SYNTHETIC BIOLOGY

Genome-scale modeling enables metabolic engineering of *Saccharomyces cerevisiae* for succinic acid production

Rasmus Agren · José Manuel Otero · Jens Nielsen

Received: 23 January 2013 / Accepted: 1 April 2013 / Published online: 23 April 2013

Abstract In this work, we describe the application of a genome-scale metabolic model and flux balance analysis for the prediction of succinic acid overproduction strategies in *Saccharomyces cerevisiae*. The top three single gene deletion strategies, Δ*mdh1*, Δ*oac1*, and Δ*dic1*, were tested using knock-out strains cultivated anaerobically on glucose, coupled with physiological and DNA microarray characterization. While Δ*mdh1* and Δ*oac1* strains failed to produce succinate, Δ*dic1* produced 0.02 C-mol/C-mol glucose, in close agreement with model predictions (0.03 C-mol/C-mol glucose). Transcriptional profiling suggests that succinate formation is coupled to mitochondrial redox balancing, and more specifically, reductive TCA cycle activity. While far from industrial titers, this proof-of-concept suggests that *in silico* predictions coupled with experimental validation can be used to identify novel and non-intuitive metabolic engineering strategies.

Keywords Succinic acid · Metabolic engineering · Genome-scale modeling · DNA microarrays · *Saccharomyces cerevisiae*

Electronic supplementary material The online version of this article (doi:10.1007/s10295-013-1269-3) contains supplementary material, which is available to authorized users.

R. Agren · J. M. Otero · J. Nielsen (✉)
Department of Chemical and Biological Engineering, Chalmers University of Technology, SE-41296 Gothenburg, Sweden
e-mail: nielsenj@chalmers.se

Present Address:
J. M. Otero
Vaccine and Biologics Process Development, Bioprocess Research and Development, Merck Research Labs, West Point, PA, USA

Introduction

The chemical manufacturing industry is actively seeking cost-effective, environmentally friendly, renewable, and sustainable raw material feedstocks that will not only enable production of key chemical building blocks, but can serve as a platform for future products [32]. In 2004, the US Department of Energy identified succinic acid as an added-value chemical building block, with an estimated 15,000 t/year world-wide demand. The demand is predicted to expand to commodity chemical status with 270,000 t/year, representing a potential >2 billion USD annual market [26, 44]. Within microbial metabolism succinate formation results from two routes: (1) the isocitrate lyase, Icl1p, catalyzed conversion of isocitrate to equimolar glyoxylate and succinate, and (2) from the α-keto-glutarate dehydrogenase complex, Kgd1p/Kgd2p/Lpd1p, catalyzed conversion of α-keto-glutarate to equimolar succinate, with a net production of CO_2, NADH, and ATP. Succinate is subsequently depleted by the succinate dehydrogenase complex, Sdh1p/Sdh2p/Sdh3p/Sdh4p to equimolar fumarate with the net production of protonated ubiquinone [11].

Numerous industrial biotechnology efforts have focused on metabolic engineering of prokaryotes to overproduce succinic acid, including *Anaerobiospirillium succiniciproducens*, *Actinobacillus succinogenes*, *Corynebacterium glutanicum*, *Mannheimia succiniciproducens*, *Prevotella ruminocola*, *Succinivibrio dextrinosolvens*, and a metabolically engineered succinic acid over-producing *Escherichia coli*, have been presented [40]. These hosts all grow at neutral pH, which results in secretion of the salt form, succinate, rather than the acid form. This in turn requires a costly acidification and precipitation step to produce succinic acid, which is the desired product. This is a general

concern when using microbial cell factories for the production of organic acids [38].

Saccharomyces cerevisiae represents a well-established, generally regarded as safe, robust, scalable industrial production host capable of growth on diverse carbon sources, chemically defined medium, both aerobic and anaerobic, and with a wide pH operating range (3.0–6.0). However, unlike the bacterial hosts described above, succinate does not natively accumulate in *S. cerevisiae*. There has so far been limited work on metabolic engineering of *S. cerevisiae* for production of succinic acid for industrial applications. Succinic acid production in genetically modified sake yeast strains has been demonstrated for modification of taste profiles, primarily focusing on multi-gene deletions of citric acid cycle enzymes aconitase (Aco1p), fumarate reductase (Osm1p), α-ketoglutarate dehydrogenase (Kgdp), fumarase (Fum1), and succinate dehydrogenase (Sdh1), resulting in <0.7 g L^{-1} succinic acid on complex medium [5, 6, 22]. There has also been significant experimental work focused on elucidating the physiological role of cytosolic and mitochondrial fumarate reductase (Frd1p and Osm1p, respectively) in the context of facilitating anaerobic fermentation of *S. cerevisiae* [4, 9, 13]. Significant effort has been applied to understand succinate formation in *S. cerevisiae* by exploring *SDH1* and *SDH3* deletion mutants, specifically using ^{13}C-NMR analysis of ^{13}C-labelled aspartate and glutamate supplemented anaerobic glucose fermentations, and DNA microarray analysis of aerobic and anaerobic glucose supplemented fermentations, respectively [10, 12]. In both efforts, no significant succinate accumulation was observed through simple deletion of the primary succinate consuming reaction, catalyzed by the succinate dehydrogenase complex. The most successful metabolic engineering attempt to date has been by Raab et al. [37]. They pursued an oxidative production route for succinate by a quadruple deletion of *SDH1*, *SDH2*, *IDP1*, and *IDH1*. This results in an interrupted TCA cycle and flux being redirected through the glyoxylate cycle instead. Following this approach they could demonstrate a 0.07 C-mol/C-mol glucose succinate yield.

Genome-scale metabolic models (GEMs), extensively described and reviewed elsewhere [23, 29, 36], provide a quantitative framework for stoichiometric biochemical models annotated with gene identity, coupled with mass-balance boundary conditions, to enable simulations of how the metabolic network operates under different conditions. For *S. cerevisiae*, the most well characterized eukaryote in systems biology, a number of GEMs have been developed. The models differ in scope, compartmentalization and intended applications [30]. The GEMs have been widely used to identify metabolic engineering targets *in silico*, e.g., by using an evolutionary programming method and flux balance analysis (FBA) for identification of multiple knockout targets [35]. Otero et al. [31] recently applied this method for the identification of sets of gene deletions which would link succinate production to growth in *S. cerevisiae*. The proposed strategy relies on a triple deletion of *SDH1*, *SER3*, and *SER33*, which leads to disabled serine synthesis from glycolysis. Since serine is required for growth it must then be synthesized from glycine. Glycine production, in turn, is coupled to succinate production through the glyoxylate shunt. Following this strategy, the authors reported a succinate yield of 0.02 C-mol/C-mol glucose, but the strain relied on glycine supplementation. Adaptive evolution followed by additional metabolic engineering steps resulted in a succinate yield of 0.05 C-mol/C-mol glucose without the need for glycine supplementation.

Here we use FBA to explore succinic acid overproduction strategies based on single and double gene deletions. Unlike the previously mentioned studies, we focus primarily on anaerobic fermentation conditions, since it is a significant advantage from an industrial viewpoint to be able to run fermentations anaerobically. The top three single gene deletion strategies, identified under anaerobic glucose fermentation conditions, were experimentally evaluated. Furthermore, these three strains were physiologically and transcriptionally characterized with the objective of gaining further knowledge into the C4 acid production by *S. cerevisiae*.

Materials and methods

Modeling

The iFF708 GEM was used for all simulations [15]. We chose to use iFF708 even though there are more recent GEMs available. This was because we believed that the relative small number of subcellular compartments and the focus on central carbon metabolism made it the most suited model for studying succinate production. The following compounds are necessary for growth in iFF708 and were unconstrained in all simulations: ammonia, phosphate, and sulfate. Ergosterol and zymosterol are necessary for growth under anaerobic conditions but were unconstrained in all simulations. A maintenance ATP requirement of 1 mmol/g-DCW/h was used, following the calculations in Forster et al. [15]. Unless otherwise stated, all simulation conditions shared an identical objective function: maximizing growth under a limiting glucose uptake rate. The glucose uptake rate, based on experimentally determined glucose uptake rates of the *S. cerevisiae* CEN.PK113-7D under batch aerobic glucose fermentation conditions (see Table 2), was fixed to 15.2 C-mmol/g-DCW/h (91.2 mmol/g-DCW/h). For simulations

referred to as *aerobic* or *semi-aerobic* the oxygen uptake rate, r_{O_2}, was unconstrained or constrained to 1.8 mmol O_2/g-DCW/L, respectively. For simulations referred to as *anaerobic*, the r_{O_2} was constrained to 0.016 mmol O_2/g-DCW/L, rather than strictly zero. This was because a small succinate production, 0.003 C-mol/C-mol glucose, is predicted under anaerobic conditions. If succinate production is constrained to zero the model predicts no growth. However, this behavior is not seen experimentally. In the model this is because the production of orotate from dihydroorotate, catalyzed by dihydroorotate dehydrogenase (encoded by *URA1*) and required for pyrimidine synthesis, is coupled to the reduction of ubiquinone to ubiquinol. Under aerobic conditions oxygen serves as the final electron acceptor and enables ubiquinone regeneration, while under anaerobic conditions, flavin adenine dinucleutoide (FAD) serves as the electron acceptor for ubiquinone regeneration. The FAD must then be regenerated by the transfer of electrons to fumarate, producing succinate. Given that experimentally it would be difficult to ensure 0 mmol O_2, potential gene deletions were, therefore, screened for micro aerobic conditions, where r_{O_2} was constrained to 0.016 mmol O_2/g-DCW/h, which was the minimum r_{O_2} required for sustaining cell growth at the same rate regardless of whether succinate production is constrained to zero or unconstrained.

The gene deletions were tested for using a brute force approach where all combinations of single or double deletions were evaluated, rather than by using a faster algorithm like OptKnock [8]. This was because any deletion strategy was to be evaluated experimentally, and only single or double deletions were within the scope of this project. All simulations were carried out using the RAVEN Toolbox [1].

Strains

The reference strain *S. cerevisiae* BY4741 (*MATa; his3Δ1; leu2Δ0; met15Δ0; ura3Δ0*) and the single deletion strains were all received from the European *S. cerevisiae* Archive for Functional Analysis (Frankfurt, Germany). The reference strain *S. cerevisiae* CEN.PK113-7D (*Mat a URA3 HIS3 LEU2 TRP1 MAL2-8^C SUC2*) was received from the Scientific Research and Development GmbH (Oberursel, Germany) [41]. The single gene-deletion knock-out strains used throughout this study and their corresponding genotype are presented in Table 1.

Medium formulation

A chemically defined minimal medium of composition 5.0 g L^{-1} $(NH_4)_2SO_4$, 3.0 g L^{-1} KH_2PO_4, 0.5 g L^{-1} $MgSO_4 \cdot 7H_2O$, 1.0 mL L^{-1} trace metal solution, 300 mg L^{-1} uracil, 800 mg L^{-1} lysine, 200 mg L^{-1} histidine, 200 mg L^{-1} methionine, 0.05 g L^{-1} antifoam 204 (Sigma-Aldrich A-8311), and 1.0 mL L^{-1} vitamin solution was used for all shake flask and 2 L well-controlled fermentations [43]. The trace element solution included 15 g L^{-1} EDTA, 0.45 g L^{-1} $CaCl_2 \cdot 2H_2O$, 0.45 g L^{-1} $ZnSO_4 \cdot 7H_2O$, 0.3 g L^{-1} $FeSO_4 \cdot 7H_2O$, 100 mg L^{-1} H_3BO_4, 1 g L^{-1} $MnCl_2 \cdot 2H_2O$, 0.3 g L^{-1} $CoCl_2 \cdot 6H_2O$, 0.3 g L^{-1} $CuSO_4 \cdot 5H_2O$, 0.4 g L^{-1} $NaMoO_4 \cdot 2H_2O$. The pH of the trace metal solution was adjusted to 4.00 with 2 M NaOH and heat sterilized. The vitamin solution included 50 mg L^{-1} d-biotin, 200 mg L^{-1} *para*-amino benzoic acid, 1 g L^{-1} nicotinic acid, 1 g L^{-1} Ca·pantothenate, 1 g L^{-1} pyridoxine HCl, 1 g L^{-1} thiamine HCl, and 25 mg L^{-1} m·inositol. The pH of the vitamin solution was adjusted to 6.5 with 2 M NaOH, sterile-filtered and the solution was stored at 4 °C. The final formulated medium, excluding glucose and vitamin solution supplementation, is adjusted to pH 5.0 with 2 M NaOH and heat sterilized. For carbon-limited cultivations the sterilized medium is supplemented with 20 g L^{-1} glucose, heat sterilized separately, and 1.0 mL L^{-1} vitamin solution is added by sterile filtration (0.20 μm pore size Ministart®-Plus Sartorius AG, Goettingen, Germany). For anaerobic fermentations a total of 4 g L^{-1} ergosterol and 168 g L^{-1} Tween 80 dissolved in pure ethanol was supplemented.

Table 1 *S. cerevisiae* strain description and genotype

Strain name	Strain genotype	Source
CEN.PK113-7D	*MATa URA3 HIS3 LEU2 TRP1 SUC2 MAL2-8^C*	SRD GmbH[a]
Reference (REF)	BY4741: *MATa; his3Δ1; leu2Δ0' met15Δ0; ura3Δ0*	EUROSCARF[b]
Δ*MDH1*	BY4741: *MATa; his3Δ1; leu2Δ0; met15Δ0; ura3Δ0; YKL085w:kanMX4*	
Δ*OAC1*	BY4741: *MATa; his3Δ1; leu2Δ0; met15Δ0; ura3Δ0; YKL120w:kanMX4*	
Δ*DIC1*	BY4741: *MATa; his3Δ1; leu2Δ0; met15Δ0; ura3Δ0; YLR348c:kanMX4*	
Δ*SDH3*[b]	BY4743: *MATa/α; his3Δ1/ his3Δ1; leu2Δ0/ leu2Δ0; met15Δ0/ met15Δ0; ura3Δ0/ ura3Δ0; YKL141w:kanMX4/YKL141w*	

All strains were haploid of mating type a, with the exception of the Δ*SDH3* strain, which is diploid and mating type a/α. A haploid strain of Δ*SDH3* was reported as not viable

[a] Scientific Research and Development GmbH (Oberursel, Germany)

[b] European *S. cerevisiae* Archive for Functional Analysis (Frankfurt, Germany)

Shake flask cultivations and stirred tank fermentations

Shake flask cultivations were completed in 500 mL Erlenmeyer flasks with two diametrically opposed baffles and two side-necks with septums for sampling by syringe. Flasks were heat sterilized with 100 mL of medium, inoculated with a single colony, and incubated at 30 °C with orbital shaking at 150 rpm. Stirred tank fermentations were completed in well-controlled, aerobic or anaerobic, 2.2 L Braun Biotech Biostat B fermentation systems with a working volume of 2 L (Sartorius AG, Goettingen, Germany). The temperature was controlled at 30 °C. The fermenters were outfitted with two disk-turbine impellers rotating at 600 rpm. Dissolved oxygen was monitored with an autoclavable polarographic oxygen electrode (Mettler-Toledo, Columbus, OH, USA). During aerobic cultivation the air sparging flow rate was 1 vvm. During anaerobic cultivation nitrogen containing less than 5 ppm O_2 was used for sparging at a constant flow rate of 2 vvm, with less than 1 % air saturated oxygen in the fermenter as confirmed by dissolved oxygen and off-gas analysis. The higher flow rate of 2 vvm was employed to ensure anaerobic conditions; however, it is acknowledged that ethanol stripping was likely to increase. The pH was kept constant at 5.0 by automatic addition of 2 M KOH. Off-gas passed through a condenser to minimize the evaporation from the fermenter. The fermenters were inoculated from shake flask preculture to an initial OD_{600} 0.005.

Fermentation analysis

Off-gas analysis

The effluent fermentation gas was measured every 30 s for determination of O_2 (g) and CO_2 (g) concentrations by the off-gas analyzer Brüel and Kjær 1308 (*Brüel & Kjær*, Nærum, Denmark).

Biomass determination

The optical density (OD) was determined at 600 nm using a Shimadzu UV mini 1240 spectrophotometer (*Shidmazu* Europe GmbH, Duisburg, Germany). Duplicate samples were diluted with deionized water to obtain OD_{600} measurements in the linear range of 0–0.4 OD_{600}. Samples were always maintained at 4 °C post-sampling until OD_{600} and dry cell weight (DCW) measurements were performed. The DCW measurements were determined through the exponential phase, until stationary phase was confirmed according to OD_{600} and off-gas analysis. Nitrocellulose filters (0.45 μm Sartorius AG, Gottingen, Germany) were used. The filters were pre-dried in a microwave oven at 150 W for 10 min, and cooled in a desiccator for 10 min. Then 5.0 mL of fermentation broth were filtered, followed by 10 mL DI water. Filters were then dried in a microwave oven for 20 min at 150 W, cooled for 15 min in a desiccator, and the mass was determined.

Metabolite concentration determination

All fermentation samples were immediately filtered using a 0.45 μm syringe-filter (Sartorius AG, Gottingen, Germany) and stored at −20 °C until further analysis. Glucose, ethanol, glycerol, acetate, succinate, pyruvate, fumarate, citrate, oxalate, and malate were determined by HPLC analysis using an Aminex HPX-87H ion-exclusion column (Bio-Rad Laboratories, Hercules, CA, USA). The column was maintained at 65 °C and elution performed using 5 mM H_2SO_4 as the mobile phase at a flow rate of 0.6 mL min^{-1}. Glucose, ethanol, glycerol, acetate, succinate, citrate, fumarate, malate, oxalate were detected on a Waters 410 differential refractometer detector (Shodex, Kawasaki, Japan), and acetate and pyruvate were detected on a Waters 468 absorbance detector set at 210 nm.

Transcriptomics

RNA sampling and isolation

Samples for RNA isolation from the late-exponential phase of glucose-limited batch cultivations were taken by rapidly sampling 25 mL of culture into a 50 mL sterile Falcon tube with 40 mL of crushed ice in order to decrease the sample temperature to below 2 °C in less than 10 s. Cells were immediately centrifuged (4,000 rpm at 0 °C for 2.5 min), the supernatant discarded, and the pellet frozen in liquid nitrogen and it was stored at −80 °C until total RNA extraction. Total RNA was extracted using the FastRNA Pro RED kit (QBiogene, Carlsbad, USA) according to manufacturer's instructions after partially thawing the samples on ice. RNA sample integrity and quality was determined prior to hybridization with an Agilent 2100 Bioanalyzer and RNA 6000 Nano LabChip kit according to the manufacturer's instruction (Agilent, Santa Clara, CA, USA).

Probe preparation and hybridization to DNA microarrays

The mRNA extraction, cDNA synthesis, labeling, and array hybridization to Affymetrix Yeast Genome Y2.0 arrays were performed according to the manufacturer's recommendations (Affymetrix GeneChip® Expression Analysis Technical Manual, 2005-2006 Rev. 2.0). Washing and staining of arrays were performed using the GeneChip Fluidics Station 450 and scanning with the Affymetrix GeneArray Scanner (Affymetrix, Santa Clara, CA, USA).

Microarray gene transcription analysis

Affymetrix Microarray Suite v5.0 was used to generate CEL files of the scanned DNA microarrays. These CEL files were then processed using the statistical language and environment R v5.3 (R Development Core Team, 2007, www.r-project.org), supplemented with Bioconductor v2.3 (Biconductor Development Core Team, 2008, www.bioconductor.org) packages Biobase, affy, gcrma, and limma. The probe intensities were normalized for background using the robust multi-array average method only using perfect match (PM) probes after the raw image file of the DNA microarray was visually inspected for acceptable quality. Normalization was performed using the qspline method and gene expression values were calculated from PM probes with the median polish summary. Statistical analysis was applied to determine differentially expressed genes using the limma statistical package. Moderated t tests between the sets of experiments were used for pair-wise comparisons. Empirical Bayesian statistics were used to moderate the standard errors within each gene and Benjamini–Hochberg's method was used to adjust for multi-testing. A cut-off value of adjusted $p < 0.05$ was used for statistical significance, unless otherwise specified [39]. Gene Ontology process annotation was performed by submitting differentially expressed gene (adjusted $p < 0.05$) lists to the Saccharomyces Genome Database GO Term Finder resource and maintaining a cut-off value of $p < 0.01$ [11].

Results

Model validation and comparison to experimental data

The predictive power of the model was evaluated using fermentation data of *S. cerevisiae* CEN.PK113-7D (see Table 2). Batch aerobic and anaerobic glucose fermentations were performed in well-controlled 2 L fermentations, and compared to corresponding simulation conditions. The objective function, growth, was maximized while constraining glucose uptake rate, and for anaerobic conditions, constraining the oxygen uptake rate (r_{O_2}) to 0.016 mmol O_2/g-DCW/h as discussed in "Methods". Table 2 demonstrates that under aerobic conditions, 96.3 ± 4.0 % of all carbon is recovered, and distributed across ethanol (54 %), acetate (1 %), glycerol (8 %), carbon dioxide (16 %), and biomass (17 %) formation. Figure 1 shows the results of simulated carbon distributions and the specific growth rate (SGR) when oxygen was unconstrained. As can be seen there is a poor agreement with batch glucose aerobic experimental data due to the inability of the model to describe the Crabtree effect, as discussed earlier by Akesson et al. [2]. When r_{O_2} was constrained to experimentally determined fermentation values of 1.8 mmol O_2/g-DCW/h, referred to as *semi-aerobic*, the simulation accurately predicted the SGR (0.38 vs. 0.40 h^{-1}, experimental vs. simulation, respectively), ethanol yield (0.54 vs. 0.54 C-mol/C-mol glucose), and biomass yield (0.17 vs. 0.18 C-mol/C-mol glucose). However, carbon dioxide (0.16 vs. 0.30 C-mol/C-mol glucose) and glycerol (0.08 vs. 0.0 C-mol/C-mol glucose) yields were in poor agreement. While the relatively high carbon recovery observed experimentally in aerobic batch glucose fermentation suggests carbon dioxide measurements were accurate, it should be noted the theoretical ratio of carbon dioxide to ethanol production under purely fermentative glucose metabolism is 1:2, and experimentally under both aerobic, and anaerobic conditions in CEN.PK113-7D and BY4741 the ratio observed is 1:3 [27]. The original iFF708 model's ability to predict carbon dioxide production rates was validated experimentally with aerobic glucose-limited continuous cultivation data, and demonstrated an excellent fit between dilution rates 0.1 and 0.38 h^{-1}, representing a broad span of respiratory quotients [14]. This, therefore, suggests that carbon dioxide metabolism in CEN.PK113-7D and BY4741 under batch glucose fermentation conditions deviates from theoretical expectations, or when considered in the context of a highly interconnected network, not fully described by the stoichiometry of iFF708. It is not expected that the discrepancy in carbon dioxide predictive power would significantly alter the succinate overproduction strategies identified. It is further interesting to note that in the same work, the only data point not predicted by the original iFF708 was the glycerol production rate at the higher dilution rate, 0.38 h^{-1}, most representative of batch conditions [14].

Biomass formation as a result of glucose respiro-fermentative metabolism, with a high dependence on oxygen availability and glucose concentration, results in the formation of excess NADH [28]. Excess NADH, both cytosolic and mitochondrial, is a direct result of biomass required ATP generation, and compartmental redox balance is possible through cytosolic NADH dehydrogenases, the glycerol-3-phosphate shuttle, and mitochondrial redox shuttles [16, 21, 24, 33]. Glycerol formation results from redox balancing. NADH regeneration to NAD^+ in the cytosol, with subsequent glycerol production, can be reduced through expression of a cytosolic NADH oxidase [42].

Model validation was initially performed using *S. cerevisiae* CEN.PK113-7D batch glucose aerobic fermentation data; however, realizing that succinate metabolic engineering strategies would likely require exploration of anaerobic metabolism, similar comparative analysis for anaerobic fermentations was performed. More specifically,

Table 2 Physiological characterization

Strain	CEN.PK113-7D		CEN.PK113-7D		Reference (BY4741)		Δ*mdh1*		Δ*dic1*		Δ*oac1*		Δ*sdh3*
Conditions	Aerobic	± σ ($n = 2$)	Anaerobic	± σ ($n = 2$)	Anaerobic	± σ ($n = 4$)	Anaerobic	± σ ($n = 4$)	Anaerobic	± σ ($n = 4$)	Anaerobic	± σ ($n = 3$)	Anaerobic
Specific growth rate (h^{-1})	0.38	<0.00	0.29	0.01	0.28	<0.00	0.28	0.01	0.24	0.02	0.23	<0.00	0.26
Product yields (C-mol/C-mol substrate)													
Y_{SX}	0.17	0.02	0.13	0.01	0.12	0.02	0.17	0.06	0.12	0.00	0.13	0.00	0.18
Y_{SEtOH}	0.54	0.04	0.44	0.03	0.45	0.01	0.48	0.00	0.50	0.01	0.54	0.01	0.53
Y_{SCO_2}	0.16	<0.00	0.12	<0.00	0.13	0.03	0.14	0.01	0.11	0.00	0.14	0.00	0.18
Y_{SAcet}	0.01	<0.00	0.00	<0.00	0.01	0.00	0.00	0.00	0.00	0.00	0.00	0.00	0.01
Y_{SGlyc}	0.08	0.03	0.11	0.30	0.08	0.01	0.09	0.00	0.09	0.00	0.09	0.00	0.11
Y_{SSuc}	0.00	<0.00	0.00	<0.00	0.00	<0.00	0.00	<0.00	0.02	<0.00	0.00	<0.00	0.00
Y_{SPyr}	0.00	<0.00	0.00	<0.00	0.00	0.06	0.00	<0.00	0.00	<0.00	0.00	<0.00	0.00
Productivities (C-mmol/g-DCW/h)													
r_{Gluc}	91.2	6.0	93.1	4.0	89.7	2.8	68.6	18.2	74.5	2.0	73.3	3.0	68.5
r_{EtOH}	49.7	6.6	41.0	5.5	40.8	0.8	32.9	8.7	37.4	1.9	39.2	3.4	36.0
r_{CO_2}	15.4	0.0	11.1	0.0	11.3	3.3	9.7	2.1	7.9	0.1	9.9	0.1	12.0
r_{Acet}	0.7	0.3	0.4	0.1	0.3	0.4	0.3	0.1	0.2	0.1	0.3	0.1	0.4
r_{Glyc}	7.3	3.4	10.5	2.2	3.5	4.8	5.9	1.6	6.7	0.3	6.7	0.3	7.3
r_{Suc}	0.0	0.0	0.0	0.0	0.1	0.0	0.1	0.0	1.6	0.1	0.1	0.1	0.3
r_{Pyr}	0.4	0.0	0.3	0.0	0.1	0.1	0.2	0.1	0.1	0.1	0.2	0.1	0.2
r_{O_2}	1.8	0.3	0.0	0.0	0.1	0.2	0.9	0.0	0.2	0.2	0.0	0.2	0.4
Carbon recovery (%)	96.3	4.0	81.30	3.2	79.0	6.2	88.6	6.7	84.7	1.0	89.6	1.0	100.3
Succinate titer (g L^{-1})	0.02	0.01	0.00	0.00	0.03	0.00	0.03	0.00	0.23	0.03	0.02	0.03	0.04
Biomass titer (g L^{-1})	1.96	0.08	2.00	0.12	2.05	0.13	2.07	0.198	1.97	0.00	2.08	0.00	2.23
Y_{XSuc} (g/g-biomass)	0.01	0.00	0.00	0.00	0.01	0.00	0.01	0.00	0.11	0.02	0.01	0.02	0.02

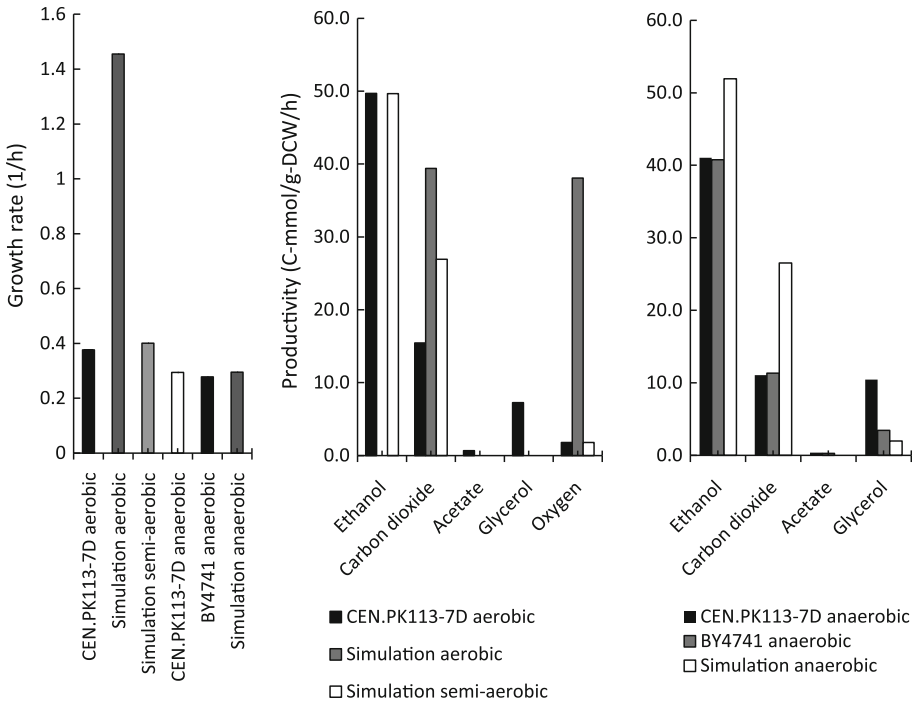

Fig. 1 Comparison between experimental and simulated fermentation data. Comparison of the SGR and specific productivities for simulated data and experimental data generated using the reference *S. cerevisiae* CEN.PK113-7D and BY4741 under aerobic and anaerobic glucose batch fermentations. For the condition, *simulation aerobic*, *simulation semi-aerobic*, *simulation anaerobic*, the r_{O_2} was unconstrained, constrained to 1.8 mmol-O_2/g-DCW/h, and constrained to 0.016 mmol-O_2/g-DCW/h, respectively. For aerobic experimental data, the specific glucose uptake rate was 91.2 C-mmol/g-DCW/h for CEN.PK113-7D. For anaerobic experimental data, the specific glucose uptake rate was 93.1 C-mmol/g-DCW/h for CEN.PK113-7D and 89.7 C-mmol/g-DCW/h for BY4741. For all simulation conditions, the glucose uptake rate was constrained to 91.2 C-mmol/g-DCW/h

the reference *S. cerevisiae* BY4741 was also included, noting that gene deletion strategies to be identified *in silico* could rapidly be evaluated in vivo using the systematic Yeast Knock-Out (YKO) library available from the Saccharomyces Gene Deletion Project [45]. Under anaerobic conditions, the carbon recovery for both strains CEN.PK113-7D and BY4741 are significantly less compared to aerobic conditions (Table 2); however, when evaluating experimental and simulation values for SGR and specific productivities there is reasonable agreement. Specifically, for CEN.PK113-7D, BY4741, and anaerobic simulations the SGR was 0.29, 0.27, and 0.29 h^{-1}, respectively. For ethanol (41.0, 40.8, 51.9 C-mmol/g-DCW/h), glycerol (10.5, 3.5, 2.0 C-mmol/g-DCW/h), and carbon dioxide (11.1, 11.3, 26.5 C-mmol/g-DCW/h) specific productivities the agreement between experimental and model simulations were fair, but indicating that the lack of carbon recovery is likely a result of ethanol stripping and evaporation from the bioreactor. Emphasis was, therefore, placed on ensuring simulation conditions and constraints captured experimentally observed metabolite production, with less focus on matching exact flux values.

Gene deletion strategies for succinate overproduction

Overproduction of succinic acid was evaluated *in silico* using the various simulation conditions previously described. Prior to investigating those results, the maximum theoretical yield of succinic acid was determined *in silico*. Assuming 1 mmol ATP/g-DCW/h maintenance cost and a 10 mmol glucose/g-DCW/h uptake rate, the maximum succinate yield is 0.51 g/g-glucose. This maximum yield is based on FBA when H^+ was balanced. The exact mechanism by which succinate is transported across the cytosolic membrane has yet to be clearly elucidated, with literature suggesting both dicarboxylic acid proton-coupling, and the absence of such coupling [3]. If H^+ is treated as an external metabolite (e.g., unconstrained), the maximum yield of succinate is 0.98 g/g-glucose. Furthermore, if carbon dioxide uptake is permitted, enabling carboxylation reactions, the maximum theoretical yield is 1.124 g/g-glucose. Given the lack of physiological characterization of succinate transport, and the relatively high impact of assumptions surrounding H^+ balancing, external H^+ was balanced throughout all simulations, and the maximum succinate yield was assumed to be 0.51 g/g-glucose (0.52 C-mol/C-mol

glucose). This represents a worst case scenario in terms of the theoretical potential for *S. cerevisiae* to stoichiometrically overproduce succinate.

Under aerobic conditions there are no single gene deletions that result in increased succinate production (see Online Resource Table 1). Interestingly, the reference case simulation under aerobic conditions with no gene deletions produces a small amount of succinate (0.003 C-mol/C-mol glucose), which is not observed experimentally. If succinate excretion is constrained to zero then optimization of growth results in a similar growth rate but while producing glycerol, under minimal amounts of oxygen, and then acetate under increasing amounts of oxygen. However, experimentally, both glycerol and acetate production are observed while succinate production is absent. Under aerobic conditions, there is a strong sensitivity of succinate yield on substrate to r_{O_2} and for $r_{O_2} > 2$ mmol O_2/g-DCW/h, the succinate yield on substrate is zero (to be discussed later).

Under aerobic conditions double gene deletions only resulted in minor improvement of succinate production (data not shown). Nearly all of the predictions required the deletion of the succinate dehydrogenase complex (Sdh3p), which catalyzes the conversion of succinate to fumarate in the TCA cycle, and represents the primary succinate consumption reaction in *S. cerevisiae* central carbon metabolism. In addition to previous work suggesting that succinate dehydrogenase complex interruption does not lead to succinate accumulation [10, 12]. Table 2 confirms that deletion Δ*sdh3* in the BY4741 strain also fails to accumulate succinate.

Table 3 presents the top single gene deletions for succinate overproduction under anaerobic conditions. It shows that a significant increase in the succinate yield, by a factor of approximately tenfold from the simulated reference case, can be obtained for the single gene deletions Δ*oac1*, Δ*mdh1*, and Δ*dic1* (0.033 vs. 0.003 C-mol/C-mol glucose, single gene deletion vs. reference case simulation, respectively). Furthermore the significant increase in succinate yield on substrate resulted in nearly no impact on growth rate (0.28 vs. 0.30 h^{-1}, single gene deletion vs. reference case simulation, respectively). Physiologically, it was confirmed that Δ*oac1*, Δ*mdh1*, and Δ*dic1* are viable null mutants, and their annotation is well known, encoding for an inner mitochondrial membrane transporter (OAC1p), malate dehydrogenase (MDH1p), and an inner dicarboxylate mitochondrial transporter (DIC1p), respectively [11]. Interestingly, further simulations of the best double gene deletions resulted in the same order of magnitude succinate yields on substrate compared to the aforementioned single gene deletions.

Table 3 Top gene deletions under anaerobic constraints for succinate yield

Simulation conditions	Genotype	Specific growth rate (h^{-1})	Y_{SSuc} (C-mol/C-mol glucose)
Top single gene deletions anaerobic	No deletions	0.30	0.003
	Δoac1	0.28	0.033
	Δmdh1	0.28	0.033
	Δdic1	0.28	0.032
	Δfum1	0.30	0.005
	Δmet22	0.30	0.004
Top double gene deletions anaerobic	No deletions	0.29	0.003
	Δmdh1Δyat1	0.25	0.061
	Δmdh1Δcat2	0.25	0.061
	Δdic1Δyat1	0.25	0.060
	Δdic1Δcat2	0.25	0.060
	Δdic1Δcit2	0.25	0.056
	Δmdh1Δput2	0.26	0.051
	Δmdh1Δkgd1	0.26	0.050
	Δmdh1Δlsc2	0.26	0.050
	Δdic1Δoac1	0.25	0.051
	Δdic1Δlsc2	0.26	0.049

Physiological characterization of gene deletion strains

In order to explore and validate if the single gene deletions identified *in silico* result in more succinate production, the corresponding strains of the BY4741 background (see Table 1) were cultivated anaerobically in 2 L well controlled fermenters. Fermentation results are presented in Table 2, and comparative analysis between simulation and experimental results are presented in Fig. 2. It is seen that there is a fair agreement between model predictions and experimental data. Focusing more closely on the specific succinate productivity, the reference case, Δ*mdh1*, and Δ*oac1* experimentally determined yields are significantly lower than expected based on model simulations. The Δ*dic1* case, however, demonstrated a significantly higher yield of succinate compared to the reference case (0.02 vs. 0.00 C-mol/C-mol glucose, Δ*dic1* vs. reference, respectively), and was in-line with the *in silico* prediction (0.02 vs. 0.03 C-mol/C-mol glucose, Δ*dic1* experimental vs. Δ*dic1* anaerobic simulation, respectively). This represents a significant improvement in succinate productivity based exclusively on a novel *in silico* prediction.

Transcriptome characterization of gene deletion strains

To gain further insight into the physiological performance of each strain identified via simulation results, genome-wide DNA microarray profiling was completed under anaerobic batch glucose fermentations. Table 4 provides an overall summary of the comparative transcriptome of differentially expressed genes between Δ*dic1*, Δ*mdh1*, and Δ*oac1* strains, each compared to the reference strain. The

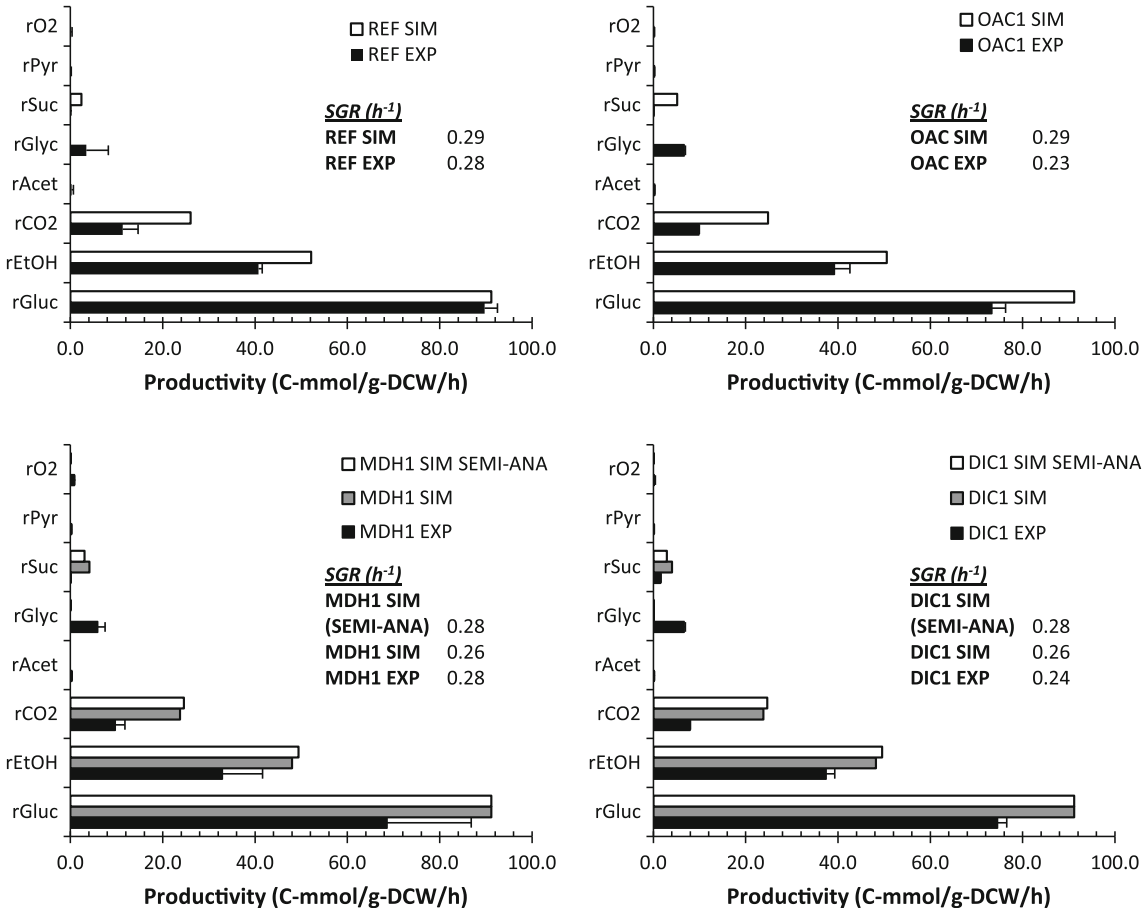

Fig. 2 Experimental and simulation comparative data for reference, Δ*oac1*, Δ*mdh1*, and Δ*dic1* strains. Summary of the SGR and specific consumption/productivity values for major carbon products (glucose, ethanol, carbon dioxide, acetate, glycerol, succinate, pyruvate, and oxygen) for both experimentally determined data of anaerobic batch glucose fermentations, and corresponding anaerobic simulation data of the BY4741 reference strain, and single gene deletion strains Δ*mdh1*, Δ*dic1*, and Δ*oac1*. In general, the experimental data suggests a lower SGR compared to the predicted growth rate, whether anaerobic simulations (referred to as *SIM*) or semi-anaerobic simulations (referred to as *SIM SEMI-ANA*) are considered. The simulation data for Δ*mdh1* and Δ*dic1* conditions attempt to highlight the significant sensitivity to relatively small changes in r_{O_2}, where the *SIM SEMI-ANA* simulation constrains r_{O_2} to 0.02 mmol O_2/g-DCW/L compared to 0 mmol O_2/g-DCWL/L, while impacting growth rate significantly. Both glucose and oxygen are consumed; however, they are presented as positive values. Succinate production was noted under all simulated conditions. However, it was only observed under the Δ*dic1* experimental condition

Table 4 Summary of differentially expressed genes

Comparative transcriptome	ΔDIC1 versus REF ($n = 2$)	ΔMDH1 versus REF ($n = 2$)	ΔOAC1 versus REF[a] ($n = 2$)
No. differentially expressed genes (p value$_{BH} < 0.01$)	117	209	5
Up-regulated	39	49	3
Down-regulated	78	160	2
Average log-fold change (±SD)			
Up-regulated	1.45 (1.61)	1.09 (0.60)	–
Down-regulated	−1.98 (1.53)	−1.55 (1.23)	–

[a] For the comparison of ΔOAC1 versus REF, the p value$_{BH} < 0.1$ criteria was applied and resulted in only 5 differentially expressed genes. Given the low number of differentially expressed genes, no average log-fold change is reported

number of differentially expressed genes for the Δ*oac1* strain compared to the reference strain was very low, and consequently suggests that deletion of Δ*oac1* causes virtually no transcriptional, and consequently, physiological differences compared to the reference BY4741 strain. The Δ*dic1* and Δ*mdh1* strains, compared to the reference strain, had 117 and 209 differentially expressed genes, respectively. Of these genes a total of 33 and 23 % were up-regulated genes and 66 and 76 % were down-regulated genes, for the Δ*dic1* and Δ*mdh1* strains, respectively. The average fold change of differentially expressed genes for the Δ*dic1* strain, both up- and down-regulated, was ≈2.5-fold greater than Δ*mdh1*. Given the relatively low differential expression for the Δ*oac1* strain, no further analysis of the transcriptional data was performed for this strain.

Table 5 Process gene ontology annotation of differentially expressed genes of ΔDIC1:REF and ΔMDH1:REF

Gene ontology	Genes annotated in Δ*dic1*	Genes annotated in Δ*mdh1*	*p* value Δ*dic1*	*p* value Δ*mdh1*
Mitochondrial electron transport, cytochrome *c* to oxygen	COX4, COX6, CYC1, COX7, COX5A	COX4, COX6, CYC1, COX7, COX5A	1.20E − 04	4.75E − 03
Electron transport chain	COX4, QCR10, COX6, CYC1, COX7, COX5A	COX4, QCR10, COX6, CYC1, COX7, COX5A, QCR2	5.80E − 04	3.04E − 03
Respiratory electron transport chain	COX4, QCR10, COX6, CYC1, COX7, COX5A	COX4, QCR10, COX6, CYC1, COX7, COX5A, QCR2	5.80E − 04	3.04E − 03
ATP synthesis coupled electron transport	COX4, QCR10, COX6, CYC1, COX7, COX5A	COX4, QCR10, COX6, CYC1, COX7, COX5A, QCR2	5.80E − 04	3.04E − 03
Mitochondrial ATP synthesis coupled electron transport	COX4, QCR10, COX6, CYC1, COX7, COX5A	COX4, QCR10, COX6, CYC1, COX7, COX5A, QCR2	5.80E − 04	3.04E − 03
Oxidation reduction	COX4, QCR10, COX6, CYC1, COX7, COX5A	COX4, QCR10, COX6, CYC1, COX7, COX5A, QCR2	5.80E − 04	3.04E − 03
Sterol transport	–	SWH1, SUT1, PDR11, DAN1, AUS1, HES1, SUT2	–	5.14E − 05
Energy derivation by oxidation of organic compounds	–	PET9, HOR2, BMH1, COX4, COX13, QCR10, COX6, PIG2, CYC1, MDH1, PET10, PUF3, NDE1, COX7, COX5A, QCR2	–	1.84E − 03
Generation of precursor metabolites and energy	–	PET9, HOR2, BMH1, HXK1, COX4, COX13, QCR10, COX6, PIG2, CYC1, MDH1, PET10, PUF3, NDE1, COX7, COX5A, PFK27, QCR2	–	2.65E − 03
Lipid transport	–	SWH1, SUT1, PDR11, DAN1, AUS1, HES1, FAA1, SUT2	–	2.94E − 03

The differentially expressed genes sets for Δ*dic1* and Δ*mdh1* were submitted for gene ontology (GO) process annotation. Table 5 presents the statistically significant GO process annotation terms, showing a high degree of similarity for the two strains, with changes mainly in genes involved in energy metabolism and electron transport. It's particularly interesting to note that there is a large overlap for the two strains and there were only four GO process categories that were unique to Δ*mdh1* as compared to Δ*dic1*, and these are involved in sterol transport, lipid transport, generation of precursor metabolites and energy, and energy derivation by oxidation of organic compounds.

Given the high degree of similarity in the GO process annotation for both the Δ*dic1* and Δ*mdh1* conditions, the complete list of differentially expressed genes were submitted for metabolic pathway annotation using the SGD Pathway Expression Viewer and Reactome databases [25, 34]. The results are presented in Online Resource Table 2 with color coding of genes according to their log-fold change and direction of expression relative to the reference case. Only a relatively small number of metabolic genes are identified in Δ*dic1* and Δ*mdh1* compared to the reference; a total of 10 and 20 genes, respectively. Perhaps more striking is that there is an overlap of nine metabolic pathway genes between both Δ*dic1* and Δ*mdh1*. The only differentially expressed gene present in the Δ*dic1* condition, not present in the Δ*mdh1* condition, is Δ*dic1*.

Discussion

Succinic acid overproduction metabolic engineering strategies in *S. cerevisiae* are limited. The most successful metabolic engineering strategy to date relies on oxidative production of succinate and is based on a quadruple gene deletion, with the aim of redirection of flux from the TCA cycle to the glyoxylate cycle [37]. Here we evaluated specifically anaerobic growth conditions, and the top single gene deletion targets identified resulted in significantly higher succinate yields on substrate. However, the yield was not as high as what was reported using the oxidative route (0.02 vs. 0.07 C-mol/C-mol glucose).

As discussed in the Introduction, a recent paper by Otero et al. [31] also makes use of FBA for the purpose of succinate production in *S. cerevisiae*. Attempts to reproduce those simulations resulted in significantly reduced succinate yield,

and could only be obtained if a constraint preventing acetaldehyde secretion was imposed (data not shown). The underlying reason for this was that threonine aldolase was erroneously assigned to be irreversible in the direction of glycine and acetaldehyde to threonine in the original version of iFF708. In later models, and in the iFF708 version which we used, this has been corrected to be in the opposite direction [19]. This in turn provides a metabolic route for synthesis of serine from threonine, and, therefore, uncouples serine synthesis and succinate production.

The metabolic engineering strategies identified through Δ*dic1*, Δ*mdh1*, and Δ*oac1*, suggest a common mechanism. Mitochondrial redox balance must be maintained, and while respiratory metabolic activity under anaerobic conditions is reduced compared to aerobic conditions, some activity is required to support glutamate/glutamine metabolism from α-keto-glutarate [9, 10]. This results in the production of NADH. During anaerobic metabolism, NAD^+ regeneration occurs via the following pathways according to our simulations (where the subscript *m* denotes mitochondrial):

$$\text{OAC1p} : \text{oxaloacetate} \rightarrow \text{oxaloacetate}_\text{m} + \text{H}^+_\text{m},$$

$$\text{MDH1p} : \text{oxaloacetate}_\text{m} + \text{NADH}_\text{m} \rightarrow \text{malate}_\text{m} + \text{NAD}^+_\text{m},$$

$$\text{DIC1p} : \text{malate}_\text{m} + \text{phosphate} \rightarrow \text{malate} + \text{phosphate}_\text{m},$$

$$\text{MIR1p} : \text{H}^+_\text{m} + \text{phosphate}_\text{m} \rightarrow \text{phosphate},$$

$$\text{Net reaction stoichiometry} : \text{oxaloacetate} + \text{NADH}_\text{m} \rightarrow \text{malate} + \text{NAD}^+_\text{m}.$$

In the cytosol, malate is then converted to oxaloacetate, and the resulting NADH is converted to NAD^+ with the production of glycerol. If we consequently assume that Δ*mdh1* were deleted, then NAD^+ regeneration occurs in the following manner according to the simulations:

$$\text{FUM1p} : \text{malate}_\text{m} \rightarrow \text{fumarate}_\text{m},$$

$$\text{NDIp} : \text{ubiquinone}_\text{m} + \text{NADH}_\text{m} \rightarrow \text{ubiquinol}_\text{m} + \text{NAD}^+_\text{m},$$

$$\text{SDH3p} : \text{ubiquinol}_\text{m} + \text{FAD}_\text{m} \rightarrow \text{ubiquinone}_\text{m} + \text{FADH}_{2\text{m}},$$

$$\text{OSM1p} : \text{fumarate}_\text{m} + \text{FADH}_{2\text{m}} \rightarrow \text{succinate}_\text{m} + \text{FAD}_\text{m},$$

$$\text{DIC1p} : \text{malate} + \text{succinate}_\text{m} \rightarrow \text{malate}_\text{m} + \text{succinate},$$

$$\text{Net reaction stoichiometry} : \text{malate} + \text{NADH}_\text{m} \rightarrow \text{succinate} + \text{NAD}^+_\text{m}.$$

The above mechanism is highly dependent on several metabolic pathway assumptions, particularly that there are no other mitochondrial reactions capable of NAD^+_m regeneration. Also, the Δ*mdh1* strategy is highly sensitive to r_{O_2}, as shown in Fig. 3, because of the succinate production driven requirement for electron donation from

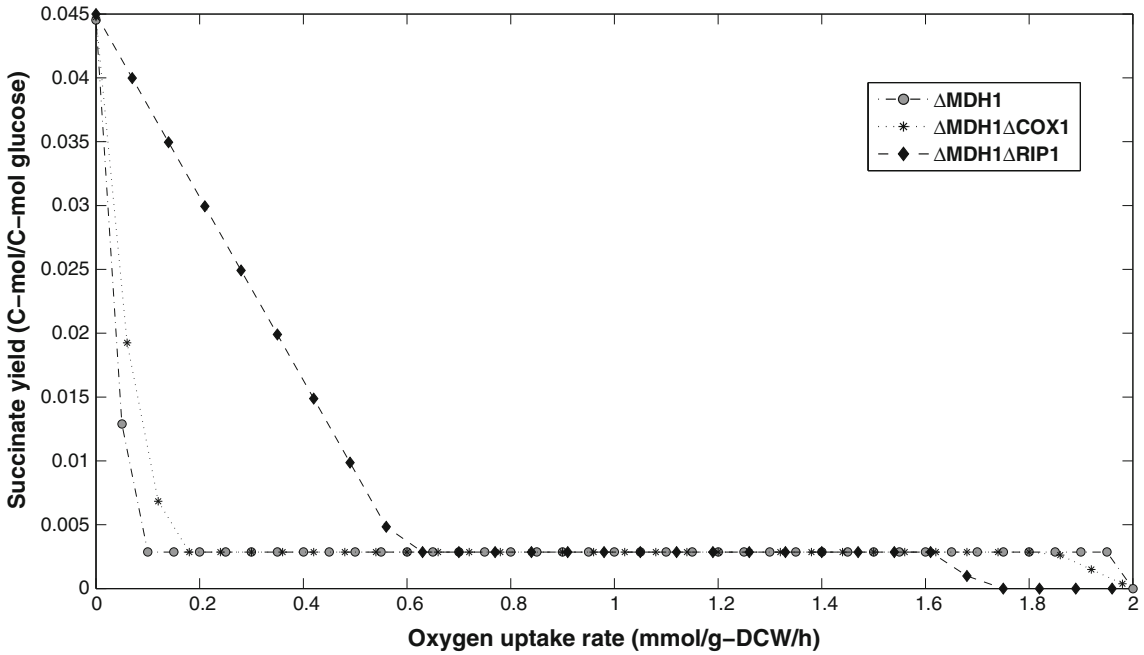

Fig. 3 Oxygen sensitivity of succinate yield on glucose. Succinate yield on glucose when r_{O_2} is constrained between 0 and 2 mmol O_2/g-DCW/h, while maximizing for growth under constrained glucose uptake rate. Data is shown for the single gene deletion of *MDH1*, the double gene deletion of *MDH1* and *COX1*, and the double gene deletion of *MDH1* and *RIP1*. The reference model has a succinate yield of approximately 0.003 C-mol/C-mol glucose (similar to the baseline seen for the three deletion strategies) up until 1.8 mmol O_2/g-DCW/h, after which is drops to zero. The *MDH1* encodes malate dehydrogenase, *RIP1* encodes ubiquinol cytochrome *c* reductase, and *COX1* encodes subunit I of the cytochrome *c* oxidase

ubiquinone to succinate and not oxygen. Even small values of r_{O_2} (<0.1 mmol O_2/g-DCW/h) result in no succinate production. If *COX1* (encoding subunit I of cytochrome *c* oxidase) and *RIP1* (encoding ubiquinol cytochrome *c* reductase) are deleted in combination with *MDH1*, to eliminate oxygen reactivity, the r_{O_2} range across which succinate yield is observed for the Δ*mdh1* strategy is extended to 0.6 mmol O_2/g-DCW/h (see Fig. 3). Furthermore, it should be noted that additional multi-gene deletion strategies leveraging the general Δ*mdh1* strategy could be expanded. A simple triple gene deletion strategy of Δ*mdh1* Δ*cat2* Δ*cit2* was simulated (data not shown), and resulted in further improved succinate yield on glucose (0.08 vs. 0.03 C-mol/C-mol glucose for only Δ*mdh1*), thee *CAT2* and *CIT2* encode carnitine acetyl-CoA transferase and citrate synthase, respectively.

The Δ*dic1* strategy, relying on deletion of the mitochondrial dicarboxylate carrier DIC1p, catalyzes the following transport reaction, noting the intermediate transport of orthophosphate:

$$\begin{aligned}&\text{Dic1}: \text{malate} + \text{succinate}_{\text{m}} \rightarrow \text{malate}_{\text{m}} + \text{succinate}\\ &(\text{malate} + \text{orthophosphate}_{\text{m}} \rightarrow \text{malate}_{\text{m}} + \text{orthophosphate})\\ &(\text{succinate} + \text{orthophosphate}_{\text{m}} \rightarrow \text{succinate}_{\text{m}} + \text{orthophosphate})\end{aligned}.$$

Assuming *DIC1* deletion, then the resulting simulated pathway is:

$$\text{NDIp}: \text{ubiquinone}_{\text{m}} + \text{NADH}_{\text{m}} \rightarrow \text{ubiquinol}_{\text{m}} + \text{NAD}^{+}_{\text{m}},$$

$$\text{SDH3p}: \text{ubiquinol}_{\text{m}} + \text{FAD}_{\text{m}} \rightarrow \text{ubiquinone}_{\text{m}} + \text{FADH}_{2\text{m}},$$

$$\text{FRDS1p}: \text{fumarate} + \text{FADH}_{2\text{m}} \rightarrow \text{succinate} + \text{FAD}_{\text{m}},$$

$$\text{Net reaction stoichiometry}: \text{fumarate} + \text{NADH}_{\text{m}} \rightarrow \text{succinate} + \text{NAD}^{+}_{\text{m}}.$$

The Δ*dic1* strategy relies heavily on the sub-cellular localization and function of FRDS1p, soluble mitochondrial fumarate reductase, which continues to be poorly understood. However, recent work has suggested that a double deletion *S. cerevisiae* mutant, Δ*osm1* Δ*frds1*, failed to grow under batch glucose anaerobic conditions. Furthermore, during anaerobic growth, *FRDS1* expression in the wild-type was two to eight times higher than that of *OSM1*, suggesting that formation of succinate is strictly required for the re-oxidation of $FADH_2$ and its expression may be oxygen-regulated [9]. While neither *FRDS1* nor *OSM1* were significantly differentially expressed in the Δ*mdh1* or Δ*dic1* mutants compared to the reference strain, *FRDS1* was slightly up-regulated in the Δ*dic1* mutant compared to the Δ*mdh1* mutant ($\log_{10}$ fold change 0.11 vs. −0.10, respectively). Lastly, as shown (see Online Resource Table 2) there was strong up-regulation of *CYC1* in both the Δ*dic1* and Δ*mdh1* mutants. *CYC1* facilitates electron transfer from ubiquinone cytochrome C oxidoreductase to cytochrome C oxidase. This direction, which is the normal oxidative route and ends in reduction of O_2, would not be possible under fully anaerobic conditions. The upregulation can therefore be viewed as a coping strategy to deal with the stress of redox imbalance. Deletion of *CYC1* could therefore be a way to ensure that all NAD^+ regeneration is coupled to succinate production. It has been well established that *CYC1* is both glucose repressed and regulated by the presence of oxygen and heme [7, 17, 18, 20]. However, this does not explain the lack of succinate production observed in the Δ*mdh1* mutant. It has been suggested that mitochondrial $FADH_2$ could be oxidized in the cytosol, which may provide an explanation for the failure of the Δ*mdh1* and Δ*oac1* mutants to produce any succinate [13]. In any event, the strategies proposed here rely on the capacity for reductive TCA cycle activity under anaerobic conditions, and more specifically, the catalysis of fumarate to succinate via fumarate reductase. There is data suggesting that *S. cerevisiae* can exhibit this metabolic state [9, 10].

In conclusion, a GEM was used to predict single deletion strategies that could lead to increased succinate production and that were physiologically feasible during anaerobic growth. Three of these strategies were validated in vivo and one, Δ*dic1*, was identified to lead to a significant improvement in succinate yield on substrate, in close agreement with the model prediction. Furthermore, physiological characterization and transcriptome analysis were used to propose biological mechanisms. The mechanisms proposed rely heavily on inter-compartmental transport reactions as well as redox balancing, both identified as the dominant GO process categories in the Δ*dic1* succinate overproducing mutant. Further in vivo characterization of the transport reactions, and subsequent corresponding modifications to the genome-scale network reconstruction would be required for further improvements and understanding of metabolic engineering strategies.

Acknowledgments José Manuel Otero was a Merck Doctoral Fellow and acknowledges financial support from Merck Research Labs, Merck & Co., Inc. We also acknowledge funding from the Knut and Alice Wallenberg Foundation and the Chalmers Foundation.

References

1. Agren R, Liu L, Shoaie S, Vongsangnak W, Nookaew I et al (2013) The RAVEN toolbox and its use for generating a genome-scale metabolic model for penicillium chrysogenum. PLoS Comput Biol. doi:10.1371/journal.pcbi.1002980
2. Akesson M, Forster J, Nielsen J (2004) Integration of gene expression data into genome-scale metabolic models. Metab Eng 6:285–293
3. Aliverdieva DA, Mamaev DV, Bondarenko DI, Sholtz KF (2006) Properties of yeast *Saccharomyces cerevisiae* plasma membrane dicarboxylate transporter. Biochemistry (Mosc) 71:1161–1169

4. Arakawa K, Yamada Y, Shinoda K, Nakayama Y, Tomita M (2006) GEM system: automatic prototyping of cell-wide metabolic pathway models from genomes. BMC Bioinform 7:168
5. Arikawa Y, Kobayashi M, Kodaira R, Shimosaka M, Muratsubaki H et al (1999) Isolation of sake yeast strains possessing various levels of succinate- and/or malate-producing abilities by gene disruption or mutation. J Biosci Bioeng 87:333–339
6. Arikawa Y, Kuroyanagi T, Shimosaka M, Muratsubaki H, Enomoto K et al (1999) Effect of gene disruptions of the TCA cycle on production of succinic acid in *Saccharomyces cerevisiae*. J Biosci Bioeng 87:28–36
7. Boss JM, Darrow MD, Zitomer RS (1980) Characterization of yeast iso-1-cytochrome *c* mRNA. J Biol Chem 255:8623–8628
8. Burgard AP, Pharkya P, Maranas CD (2003) Optknock: a bilevel programming framework for identifying gene knockout strategies for microbial strain optimization. Biotechnol Bioeng 84:647–657
9. Camarasa C, Faucet V, Dequin S (2007) Role in anaerobiosis of the isoenzymes for *Saccharomyces cerevisiae* fumarate reductase encoded by OSM1 and FRDS1. Yeast 24:391–401
10. Camarasa C, Grivet JP, Dequin S (2003) Investigation by 13C-NMR and tricarboxylic acid (TCA) deletion mutant analysis of pathways for succinate formation in *Saccharomyces cerevisiae* during anaerobic fermentation. Microbiology 149:2669–2678
11. Cherry JM, Adler C, Ball C, Chervitz SA, Dwight SS et al (1998) SGD: saccharomyces genome database. Nucleic Acids Res 26:73–79
12. Cimini D, Patil KR, Schiraldi C, Nielsen J (2009) Global transcriptional response of *Saccharomyces cerevisiae* to the deletion of SDH3. BMC Syst Biol 3:17
13. Enomoto K, Arikawa Y, Muratsubaki H (2002) Physiological role of soluble fumarate reductase in redox balancing during anaerobiosis in *Saccharomyces cerevisiae*. FEMS Microbiol Lett 215:103–108
14. Famili I, Forster J, Nielsen J, Palsson BO (2003) *Saccharomyces cerevisiae* phenotypes can be predicted by using constraint-based analysis of a genome-scale reconstructed metabolic network. Proc Natl Acad Sci USA 100:13134–13139
15. Forster J, Famili I, Fu P, Palsson BO, Nielsen J (2003) Genome-scale reconstruction of the *Saccharomyces cerevisiae* metabolic network. Genome Res 13:244–253
16. Geertman JM, van Maris AJ, van Dijken JP, Pronk JT (2006) Physiological and genetic engineering of cytosolic redox metabolism in *Saccharomyces cerevisiae* for improved glycerol production. Metab Eng 8:532–542
17. Guarente L, Lalonde B, Gifford P, Alani E (1984) Distinctly regulated tandem upstream activation sites mediate catabolite repression of the CYC1 gene of *S. cerevisiae*. Cell 36:503–511
18. Guarente L, Mason T (1983) Heme regulates transcription of the CYC1 gene of *S. cerevisiae* via an upstream activation site. Cell 32:1279–1286
19. Herrgard MJ, Swainston N, Dobson P, Dunn WB, Arga KY et al (2008) A consensus yeast metabolic network reconstruction obtained from a community approach to systems biology. Nat Biotechnol 26:1155–1160
20. Hortner H, Ammerer G, Hartter E, Hamilton B, Rytka J et al (1982) Regulation of synthesis of catalases and iso-1-cytochrome *c* in *Saccharomyces cerevisiae* by glucose, oxygen and heme. Eur J Biochem 128:179–184
21. Jagow G, Klingenberg M (1969) Hydrogen pathways in the mitochondrion of *Saccharomyces carlsbergensis*. Hoppe Seylers Z Physiol Chem 350:1155
22. Kubo Y, Takagi H, Nakamori S (2000) Effect of gene disruption of succinate dehydrogenase on succinate production in a sake yeast strain. J Biosci Bioeng 90:619–624
23. Liu L, Agren R, Bordel S, Nielsen J (2010) Use of genome-scale metabolic models for understanding microbial physiology. FEBS Lett 584:2556–2564
24. Luttik MA, Overkamp KM, Kotter P, de Vries S, van Dijken JP et al (1998) The *Saccharomyces cerevisiae* NDE1 and NDE2 genes encode separate mitochondrial NADH dehydrogenases catalyzing the oxidation of cytosolic NADH. J Biol Chem 273:24529–24534
25. Matthews L, Gopinath G, Gillespie M, Caudy M, Croft D et al (2009) Reactome knowledgebase of human biological pathways and processes. Nucleic Acids Res 37:D619–D622
26. McKinlay JB, Vieille C, Zeikus JG (2007) Prospects for a bio-based succinate industry. Appl Microbiol Biotechnol 76:727–740
27. Nielsen JH, Villadsen J, Lidén G (2003) Bioreaction engineering principles. Kluwer, New York, p 528
28. Nissen TL, Schulze U, Nielsen J, Villadsen J (1997) Flux distributions in anaerobic, glucose-limited continuous cultures of *Saccharomyces cerevisiae*. Microbiology 143(Pt 1):203–218
29. Oberhardt MA, Palsson BO, Papin JA (2009) Applications of genome-scale metabolic reconstructions. Mol Syst Biol 5:320
30. Osterlund T, Nookaew I, Nielsen J (2012) Fifteen years of large scale metabolic modeling of yeast: developments and impacts. Biotechnol Adv 30:979–988
31. Otero JM, Cimini D, Patil KR, Poulsen SG, Olsson L et al (2013) Industrial systems biology of *Saccharomyces cerevisiae* enables novel succinic acid cell factory. PLoS ONE 8:e54144
32. Otero JM, Panagiotou G, Olsson L (2007) Fueling industrial biotechnology growth with bioethanol. Adv Biochem Eng Biotechnol 108:1–40
33. Overkamp KM, Bakker BM, Kotter P, van Tuijl A, de Vries S et al (2000) In vivo analysis of the mechanisms for oxidation of cytosolic NADH by *Saccharomyces cerevisiae* mitochondria. J Bacteriol 182:2823–2830
34. Paley SM, Karp PD (2006) The pathway tools cellular overview diagram and omics viewer. Nucleic Acids Res 34:3771–3778
35. Patil KR, Rocha I, Forster J, Nielsen J (2005) Evolutionary programming as a platform for in silico metabolic engineering. BMC Bioinform 6:12
36. Price ND, Reed JL, Palsson BO (2004) Genome-scale models of microbial cells: evaluating the consequences of constraints. Nat Rev Microbiol 2:886–897
37. Raab AM, Gebhardt G, Bolotina N, Weuster-Botz D, Lang C (2010) Metabolic engineering of *Saccharomyces cerevisiae* for the biotechnological production of succinic acid. Metab Eng 12:518–525
38. Sauer M, Porro D, Mattanovich D, Branduardi P (2008) Microbial production of organic acids: expanding the markets. Trends Biotechnol 26:100–108
39. Smyth GK (2004) Linear models and empirical bayes methods for assessing differential expression in microarray experiments. Stat Appl Genet Mol Biol 3:Article3
40. Song H, Lee SY (2006) Production of succinic acid by bacterial fermentation. Enzyme Microb Technol 39:352–361
41. van Dijken JP, Bauer J, Brambilla L, Duboc P, Francois JM et al (2000) An interlaboratory comparison of physiological and genetic properties of four *Saccharomyces cerevisiae* strains. Enzyme Microb Technol 26:706–714
42. Vemuri GN, Eiteman MA, McEwen JE, Olsson L, Nielsen J (2007) Increasing NADH oxidation reduces overflow metabolism in *Saccharomyces cerevisiae*. Proc Natl Acad Sci USA 104:2402–2407
43. Verduyn C, Postma E, Scheffers WA, Van Dijken JP (1992) Effect of benzoic acid on metabolic fluxes in yeasts: a continuous-culture study on the regulation of respiration and alcoholic fermentation. Yeast 8:501–517
44. Willke T, Vorlop KD (2004) Industrial bioconversion of renewable resources as an alternative to conventional chemistry. Appl Microbiol Biotechnol 66:131–142
45. Winzeler EA, Shoemaker DD, Astromoff A, Liang H, Anderson K et al (1999) Functional characterization of the *S. cerevisiae* genome by gene deletion and parallel analysis. Science 285:901–906